JPPIPA 8(4) (2022)

Jurnal Penelitian Pendidikan IPA

Journal of Research in Science Education

http://jppipa.unram.ac.id/index.php/jppipa/index

Analysis of Image Fusion Effect in Image Quality of Kidney Stone

Fadhila Ulfa Jhora[1*], Freddy Haryanto[2], Leni Aziyus Fitri[3], Fourier Dzar Eljabbar Latief[3]

[1]Department of Physics, Universitas Negeri Padang, West Sumatera, Indonesia
[2]Department of Radiology, Baiturrahmah University, West Sumatera, Indonesia
[3]Department of Physics, Institut Teknologi Bandung, West Java, Indonesia

Received: August 30, 2022
Revised: October 27, 2022
Accepted: October 30, 2022
Published: October 31, 2022

Corresponding Author:
Fadila Ulfa Jhora
fadhila.jhora@fmipa.unp.ac.id

DOI: 10.29303/jppipa.v8i4.2208

Abstract: Kidney stones are a disease due to the buildup of substances that are not needed in the urinary system. Knowledge of the composition and type of stone is required in the treatment of action. Micro CT is one of the modalities that can be used in determining the composition of kidney stones. However, there are limitations when using single-energy micro-CT. Stone attenuation has almost the same value when using single energy, therefore it is necessary to use dual-energy CT to determine the difference in stone attenuation more precisely. The image of the dual-energy CT micro-energy stone needs to be processed before analyzing and determining the rock composition. Image fusion is one of the image processing techniques that can be used. The purpose of this study was to determine the effect of image fusion on the image quality of five kidney stones. The stages in the research carried out are collecting high energy and low energy projection image data, and performing image fusion on the two projected image data. The results obtained are first, the dual-energy CT image fusion affects the image quality which can be seen from the increase in the signal to noise ratio (SNR) value. A high SNR value provides the best image quality information.

Keywords: Kidney stones; Dual energy micro-CT; Image fusion.

Introduction

One of the common diseases found in the urinary tract is kidney stone disease (Figure 1). Kidney stones are solids that form in the urinary tract due to clumping of organic and inorganic substances that should dissolve in the urine. Kidney stones must be removed either through urine or through therapy and surgery. Before doing therapy or surgery, it is necessary to know the composition and type of kidney stones needed in determining the diagnosis and appropriate treatment.

Kidney stones are a disease due to blockage of substances in the urinary system. Substances that should be able to circulate properly in the kidneys become solids and eventually form stones as a result of this condition. Kidney stones consist of several different compositions of substances, including calcium oxalate, cystine, struvite, brushite and uric acid (UA). Calcium oxalate is the most prevalent type of kidney stone. It occurs in 70–80% of the kidney stone population (Asplin, 2002). To follow up the presence of kidney stones in patients, proper treatment is needed.

Knowledge of the composition and type of stone is needed, especially for the hospital. The importance of knowing the composition and type of stone because the treatment of kidney stone patients depends on the composition and type of stone. UA stones can be treated with alkalinization, struvite stones can be crushed by extracorporeal shock wave lithotripsy (ESWL), while brushite, calcium oxalate (CaO) and cystine stones are harder and harder to crush with ESWL (Thomas et al., 2009; Li et al., 2013). ESWL is effective and safe procedure which can be preferred in patients with ureteral stones but even these are not without some complications (Sfoungaristos, et al., 2012; Aldaqadossi, 2013). Therefore, the grouping of kidney stones is also an important thing to do regarding the diverse composition of kidney stones and the treatment measures are also adjusted to the type of stone.

How to Cite:
Jhora, F.U., Haryanto, F., Fitri, L.A., & Latief, F.D.E. (2022). Analysis of Image Fusion Effect in Image Quality of Kidney Stone. *Jurnal Penelitian Pendidikan IPA*, *8*(4), 2418–2424. https://doi.org/10.29303/jppipa.v8i4.2208

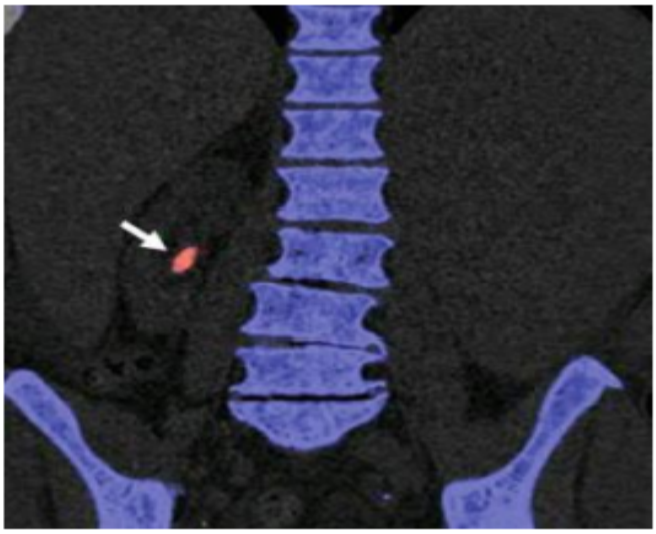

Figure 1. Coronal CT image showing the presence of kidney stones in the urinary tract (Primak, et al., 2011)

One of the modalities to determine the composition and type of kidney stones is a micro-CT scan. Research on determining the composition of kidney stones using micro-CT has been carried out previously by Leni (2015). The research conducted has succeeded in explaining the operational standards for the use (SOP) of micro-CT in determining the type of kidney stone. Studies on the characterization of kidney stones with micro-CT modalities need to be evaluated and studied further.

Single energy CT measures the attenuation of the entire energy quantity in the tissue. The attenuation value is quantized in CT number or Hounsfield unit (HU) which is then indicated by different gray level values in the image. The non-uniform composition of kidney stones causes difficulties in characterizing each component using single-energy CT. Several types of kidney stones have almost the same attenuation value even though the constituent components are not the same so it is difficult to distinguish. Therefore, single-energy CT is not appropriate for differentiating certain types of kidney stones.

The approach that can be used in dual energy CT imaging is to use DEXA. DEXA is a method used to determine the density of certain organs using dual energy X-rays. Dual energy X-rays are used to optimize the difference between soft tissue and bone tissue around organs that have different densities (Judith, 2008; Tabari et al., 2017; Chae et al., 2010). Dual-energy X-rays can also show attenuation differences that are affected by the photoelectric effect and Compton scattering in tissues with different densities (Boll et al., 2012; Zaidi, 2006). This concept is used to differentiate kidney stones using dual energy X-rays.

Boll, dual energy X-rays used are low-energy X-rays and high-energy X-rays where the energy source is obtained depending on the mechanism of the modality used. In general, there are two mechanisms used, the first mechanism uses a device with a low energy generator (70-100 kVp) and high energy (140 kVp) which is carried out alternately during the irradiation process, and the second mechanism uses a generator with a constant beam but uses a certain filter. to separate high energy and low energy (Ramos et al., 2011). In this study, stone samples were obtained from the first mechanism. Scanning is performed alternately with low energy and high energy on kidney stone samples without changing the position of the stone and other parameters (Leni, 2015).

In general, network attenuation is indicated by its CT number value. The CT number is affected by the photoelectric effect and the Compton effect, both of which also depends on the energy and the type of material being scanned. The photoelectric effect is more dominant at low energy photons and is highly dependent on the increase in photon energy while Compton scattering does not depend on photon energy. On the other hand, the photoelectric effect is also related to atomic number, while the Compton effect is more dominantly related to the density of the material (Johnson et al.,2007; Heye et al.,2012). Therefore, the effects of these two mechanisms will be different at different energy levels.

To get a combined image, it is necessary to do a series of image processing processes. One of the simple image processing processes used is image fusion. Image fusion is the process of combining images that have different parameters into a single image that is carried out simultaneously. Multi imaging fusion of medical image technologies are utilized to combine the data from many pictures to create a more useful image (Pydi et al., 2022; Fatma et al., 2016; Bikash et al., 2018). Merging is done to improve image content and image quality to make it easier to detect and identify information on the composition of kidney stones. To produce a good image quality, it is necessary to add a weight correction factor in the image summing algorithm. The weight correction factor can improve the quality of the combined image of kidney stones so that it is more informative in distinguishing kidney stones.

Image fusion is done by simulation using Matlab. The low-energy and high-energy projection images are combined into one image before reconstruction. Reconstruction is then performed on the projected image that has been combined with image fusion. Reconstruction is an important step before image analysis.

Method

The flow of research carried out is as follows (Figure 2).

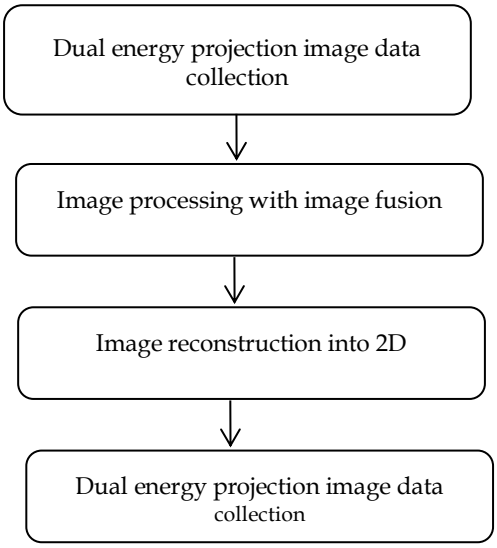

Figure 2. Flow of research

The dual energy projection image data used is a sample that has been scanned, carried out in a previous study by Leni (2015). The projection image data is the result of scanning two energy parameters on kidney stones, namely 80 kV and 120 kV, measuring 2240×2240 pixels with a depth of 16 bits. The projection image consists of five kidney stones which are scanned simultaneously with four irradiations. In the scanning process, no parameters are changed other than the voltage parameter. This information can be seen in the image parameter data log. The differences in the parameters used are described in Table 1.

The data in Table 1 collects all the parameters used when the kidney stone image is scanned using low energy and high energy. Scanning is performed alternately between low energy and high energy, without changing the position and distance of the stone to the detector and other parameters except for voltage.

Table 1. Parameters related to high energy and low energy images

Parameter	High Energy	Low Energy
Voltage	120 kV	80 kV
Current	58 µA	100 µA
Filter	AI 1 mm	AI 1 mm
Image pixel size	14.96 µm	14.96 µm
Distance from source to sample	109.2 mm	109.2 mm
Distance from detector to sample	364 mm	364 mm
Depth	16 bit	16 bit
Length of exposure	1200 ms	1000 ms
Rotation Step	0.2°	0.2°
Rotation	180°	180°

The 120 kV and 80 kV energy parameters used are the voltages set on the CT micro tool, not the average X-ray energy. To obtain the average X-ray energy at 120 kV and 80 kV irradiation, two approaches are used. The first approach uses the SpekCalc software with a 1 mm Al filter. The second approach uses the NIST spectrum reference from Bruker micro-CT skyScan 1173. The X-ray spectrum has been digitized and used as a reference in previous research by Leni (2015).

The next stage is the projection data of the two images scanned by the two energies which are combined to get a new image through the image merging process. Merging is done with Matlab simulation. The kidney stone projection image data with low energy and high energy irradiation consists of 4800 irradiation angles. Each image is combined by adding up the two projected images for each irradiation angle. Iterations are carried out until the irradiation angle is 4800.

The combined projection image resulting from image fusion is then reconstructed using nRecon software. In this study, there are five different types of projected images that have been combined with variations of the ratio in the previous stages (A, B, C, D, and E).

The reconstruction process was carried out five times with each stage consisting of one kidney stone. Each reconstruction process uses the same parameter selection for artifact correction and beam hardening. Artifact correction is selected on a scale of 20 while beam hardening correction is selected on a scale of 5. Apart from these parameters, the image window level is also set the same. The result of the reconstructed image is an image with 8.bmp format consisting of hundreds of slices for each stone.

Analysis of the effect of image fusion on the quality of the stone image is carried out by optimizing the ratio value used. The optimization steps carried out can be explained in the following steps: 1. Collect samples of the combined projection image results of six images at adjacent irradiation angles for each stone and each different ratio. 2. Analyze histograms for each projected image using ImageJ software. 3. Determine the average gray level of the image and the standard deviation of the image. 4. Calculate the SNR value of five images at the adjacent irradiation angle for each stone and each different ratio. SNR is used as a parameter to determine the image quality of each stone and optimization in the use of the ratio value. A high SNR provides the best image quality information.

Result and Discussion

The initial projection image used is a CT dual energy projection image on low energy and high energy irradiation measuring 2240×2240 pixels with a depth of 16 bits and in tiff format. Figure 3 is the projection data taken from different sources and parameters at the same irradiation angle. Figure 3 (a) is kidney stone projection data with energy irradiation of 120 kV, while Figure 3 (b)

is projection data for kidney stones with energy irradiation of 80 kV.

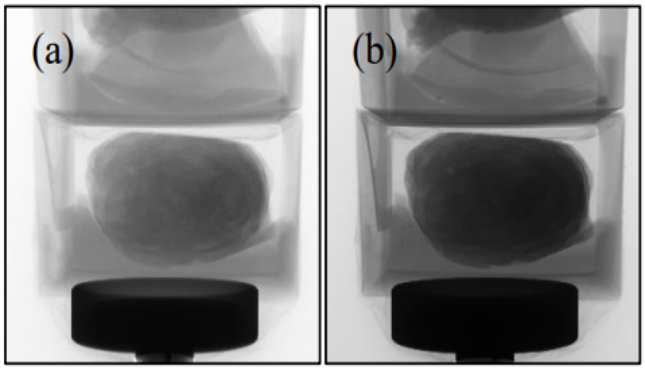

Figure 3. (a) high energy kidney stone projection image, (b) low energy kidney stone projection image.

In Figure 3 there are differences in the projection image with high energy and low energy irradiation. From the aspect of the resulting image, the projected image of stone with high energy irradiation looks whiter than the reconstructed image of stone with low energy irradiation. This shows that the signal received by the detector at high energy irradiation is greater which means that the intensity is also higher, so that the projected image looks white or brighter.

The distribution of the gray level of the image in the two-projection data can be seen from the histogram of the image. The histogram is a diagram that describes the relationship between the degree of gray in the image with a certain number of pixels. The degree of gray of each image is shown in Figure 4.

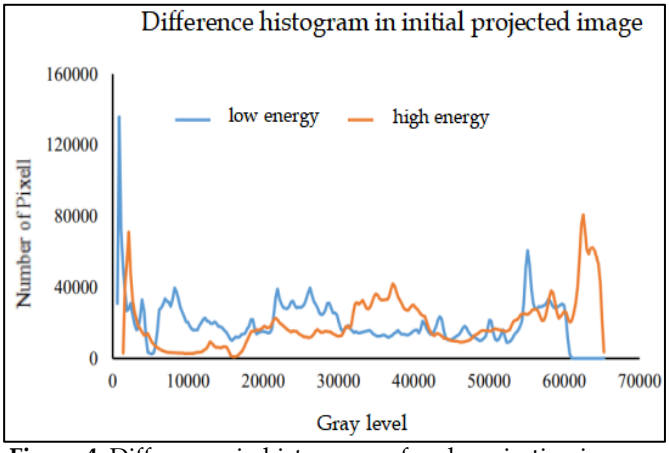

Figure 4. Differences in histograms of rock projection images with low energy and high energy

The difference between each image based on histogram data can be explained by the statistical data in Table 2 below. The initial rock projection image is an image in tiff format with a depth of 16 bits. So that the gray level of the image in Figure 6 and Table 2 below is in the range 0-65535.

Table 2. Statistical differences in the degree of gray of high energy and low energy projection images

Statistic of image gray level	Image with high energy	Image with low energy
Maximum value (max)	65535	65535
Minimum value (min)	1396	619
Average (mean)	40091.829	29172.737
Standard deviation (SD)	18639.520	18645.195

The combined projection image with image fusion is 2240×2240 pixels with a depth of 16 bits and is in tiff format. Mixed projection image of one type with different ratio variations. Each composite projection image contains information for five kidney stones. The following is an image showing a projected image of rock 1 with different ratios at a certain ROI for one of the irradiation angles (Figure 5). ROI was chosen so that the observation area is more homogeneous.

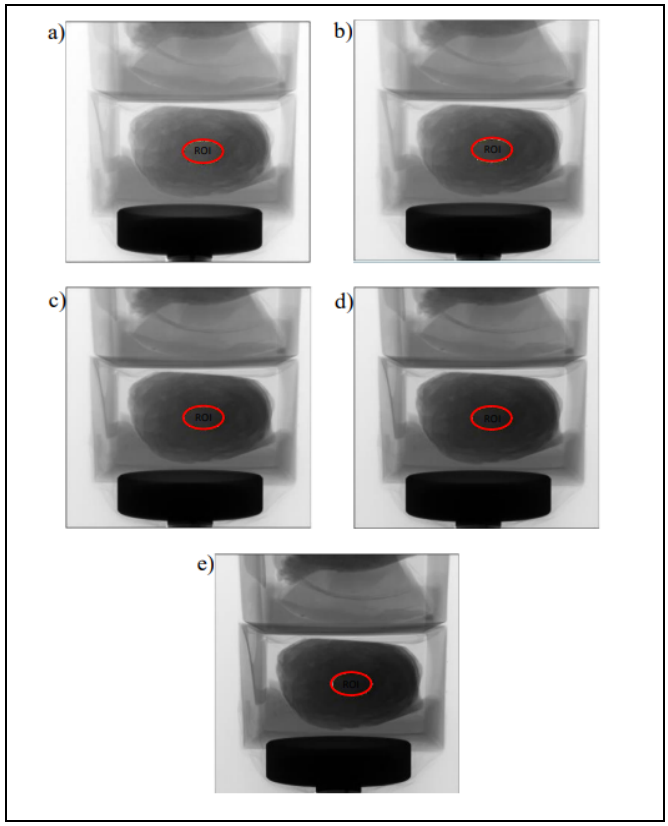

Figure 5. Combined projection image of rock 1 with variation in the ratio (a). ratio = 0, (b) ratio = 0.3, (c) ratio = 0.6, (d) ratio = 0.8, (e) ratio = 1.

The degree of gray in the image can be determined by using histogram analysis. The degree of gray in the image of stone 1 is different for each ratio value shown in Figure 6.

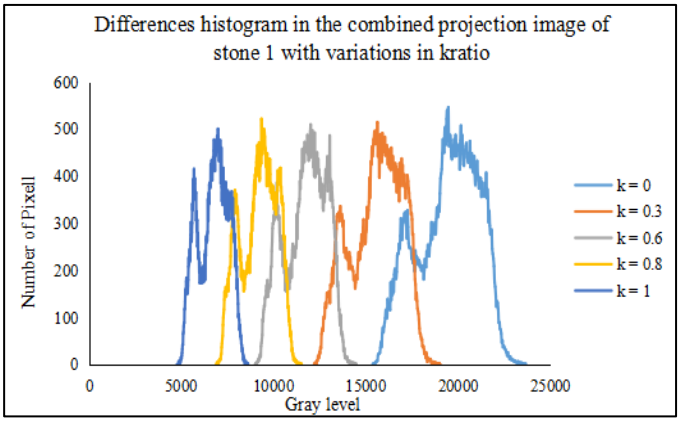

Figure 6. Comparison of histograms of composite projection images of rock 1 on ROI with a variation of ratio (a). ratio = 0, (b) ratio = 0.3, (c) ratio = 0.6, (d) ratio = 0.8, (e) ratio = 1.

The differences in each image based on histogram data can be detailed in the statistical data in Table 3 below. The combined projection image of the rock is also an image in tiff format with a depth of 16 bits. Therefore, the gray level of the image is still in the range 0-65535 as shown in Table 3.

Table 3. Statistical differences in the degree of gray of the combined projection image with the variation of the k ratio

Statistic of image gray level	k_{ratio} = 0	k_{ratio} = 0.3	k_{ratio} = 0.6	k_{ratio} = 0.8	k_{ratio} = 1
Maximum value (Max)	23701	19057	14505	11538	8634
Minimum value (Min)	15367	12197	9000	6898	4771
Average (Mean)	19464.277	15574.338	11735.592	9214, 091	6734.066
Standard deviation (SD)	1635.238	1373.538	1118.995	955.765	801.029

The deviation value or deviation of each combined projected image involving ROI shows a value that is smaller than the deviation of the initial projection image that does not involve ROI. This shows that by analyzing a certain ROI, the observation area will be more homogeneous.

The results of the combined projection image are then reconstructed to produce a 3D image and the results of the reconstructed image can be seen in Figure 7 below. The following image is a 3D image of the reconstruction of stone 1 on the first fusion (ratio = 0) of one of the slices.

The reconstructed image is an image with a .bmp format with a depth of 8 bits. The combined projection image is also reconstructed on other variations of the ratio. The difference between each reconstructed image from different ratios can be seen in the figure 8.

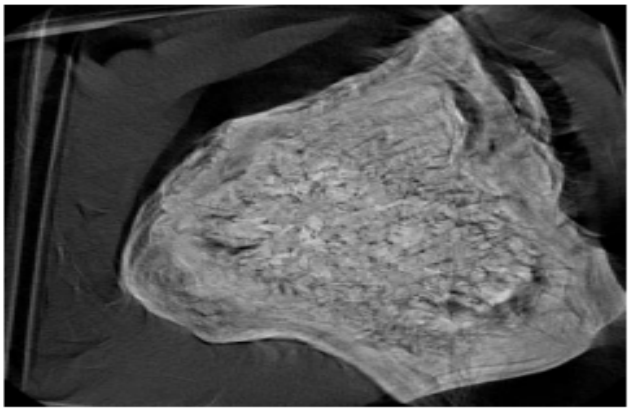

Figure 7. 3D image resulting from stone reconstruction 1 with k ratio = 0.

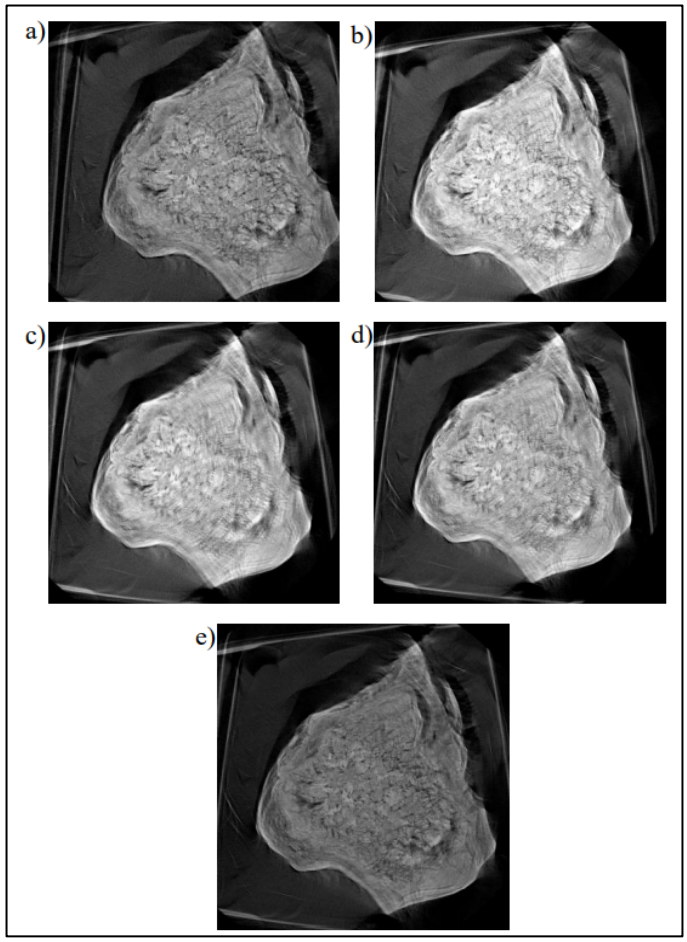

Figure 8. Differences in 3D images from the reconstruction of stone 1 with variations in the ratio (a). ratio = 0, (b) ratio = 0.3, (c) ratio = 0.6, (d) ratio = 0.8, (e) ratio = 1.

The color distribution of stone 1 in Figure 8 shows different brightness with variations in the k ratio. Stone 1 with a ratio of = 0.3 looks the brightest compared to the others. This shows that with a ratio = 0.3 the signal received by the detector is getting less, which means the more X-rays are absorbed, the intensity is lower, so the reconstructed image looks brighter. On the other hand, with the ratio = 1 stone 1 looks darkest than the others. This shows that with a ratio of 1 signal received by the detector more and more, which means that less X-rays are absorbed, the intensity is higher, so the reconstructed image looks darker than the others. The degree of gray in the image can be determined by using histogram analysis. This results were related with author Paul (2011) that proves the different weighting of the two data sets has a statistically significant effect on both the contrast enhancement and the visual quality of the fused images. The gray degree of stone reconstruction image 1 for each ratio value can be seen in Figure 9 below.

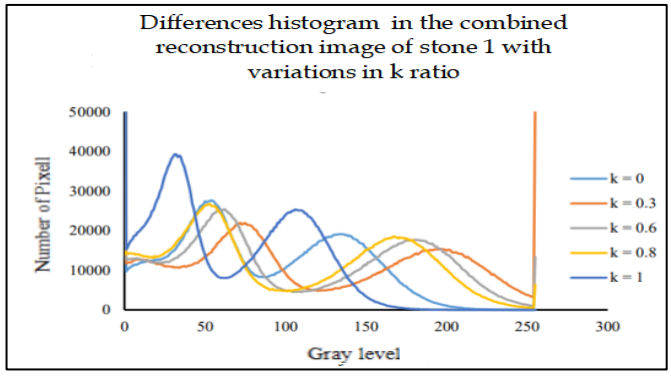

Figure 9. Comparison of histogram image reconstruction of stone 1 with the variation of ratio (a). ratio = 0, (b) ratio = 0.3, (c) ratio = 0.6, (d) ratio = 0.8, (e) ratio = 1.

The differences in each image based on histogram data are explained by statistical data in the following table. The stone reconstruction image is an image in bmp format with a depth of 8 bits. So the degree of gray in the image in Figure 9 and Table 4 is in the range of 0-255.

Table 4. Statistical differences in the degree of gray in stone reconstruction image 1 with the variation of k ratio.

Statistic of image gray level	k_{ratio} = 0	k_{ratio} = 0.3	k_{ratio} = 0.6	k_{ratio} = 0.8	k_{ratio} = 1
Maximum value (Max)	255	255	255	255	231
Minimum value (Min)	0	0	0	0	0
Average (Mean)	82.569	104.150	96,533	87.739	61.166
Standard deviation (SD)	53.022	79.683	74.439	71.650	45.045

Image fusion with variations in the ratio provides information on different degrees of gray in the five stones. The following is Table 5 which shows the comparison of the gray degrees of each stone with different ratio values. Stone histogram data was obtained from the average value of the gray degree of rock reconstruction images on six adjacent slices.

Table 5. Comparison of the average value of the stone's gray level with variations in the ratio

	k_{ratio}=0	k_{ratio}=0.3	k_{ratio}=0.6	k_{ratio}=0.8	k_{ratio}=1
Average value	147.722	199.138	190.262	175.889	108.263

The variation of the ratio gives the effect of different degrees of gray on each stone. Stone with number 1 has the highest average gray level in the ratio of 0.3. Information on the average gray level of this image cannot be used as a reference in determining which image quality is good if a different ratio is used.

SNR calculation is done to find out how it affects the image quality. The variation of the ratio value affects the image quality of kidney stone reconstruction. The parameter used in this case to determine the quality of the reconstructed image is noise. The noise parameter is seen from the SNR value of the image, where a good image has a high SNR value. The following is a table that shows the effect of the ratio value on the SNR value of kidney stone reconstruction images.

Table 6. Comparison of SNR value of stone with variations in the ratio

	k_{ratio}=0	k_{ratio}=0,3	k_{ratio}=0,6	k_{ratio}=0,8	k_{ratio}=1
SNR value	1768.194	638.741	334.436	245.709	340.116

Stone based on Table 6 has a maximum SNR value if the ratio used is 0, which means it has the best image quality if the ratio is 0.3. Increasing the weighting factor from 0.0 to 1.0, this doubles the intensity of contrast enhancement and showed the different image quality. This is in line with previous study Fidy, et al (2002) and Fatma, et al (2016), that proved fusion improve image content and image quality to make it easier to detect and identify some information.

Conclusion

In summary, image fusion dual energy micro-CT has an effect on improving the image quality of kidney

stones. Improved image quality is indicated by increasing the SNR value of rock images using different ratios. In this study explain that using different ratio in dual energy micro CT causes statistically significant changes in contrast enhancement and image quality of anatomic structures in kidney stones.A high SNR image value indicates a higher signal quality value than the noise, which means that the image quality is also better. The quality of the stone reconstruction image could be better with a ratio equal to 0.3.

References

Aldaqadossi HA. (2013). Stone expulsion rate of small distal ureteric calculi could be predicted with plasma C-reactive protein. *Urolithiasis (41)*, 235-239. https://doi.org/10.1007/s00240-013-0551-1

Asplin JR. (2002). Hyperoxaluric calcium nephrolithiasis. *Endocrinol Metab Clin North Am (31)*, 927–949. https://doi.org/10.1016/s0889-8529(02)00030-0

Bikash Meher, Sanjay Agrawal, Rutuparna Panda, Ajith Abraham. (2018). A survey on region based image fusion methods. *Journal of Information Fusion*, https://doi.org/10.1016/j.inffus.2018.07.010

Boll, D.T., Tobias Heye, Rendon C. Nelson, Lisa M. Ho, dan Daniele Marin. (2012). Dual energy CT applications in the abdomen. *American Journal of Roentgenology, 199*, S64-S70. https://doi.org/10.2214/AJR.12.9196

Chae EJ, Song JW, Krauss B, et al. (2010). Dual-energy computed tomography characterization of solitary pulmonary nodules. *J Thorac Imaging 25(4).* https://doi.org/10.1097/RTI.0b013e3181e16232.

Fatma El-Zahraa Ahmed El-Gamal, Mohammed Elmogy, Current trends in medical image registration and fusion. (2016). *Egyptian Informatics Journal 17*, 99–124. https://doi.org/10.1016/j.eij.2015.09.002

Heye, Tobias., Rendon C. Nelson., Lisa M. Ho., Daniele Marin, Daniel T. Boll. (2012). Dual energy CT applications in the abdomen. *American Journal of Roentgenology, 199*, 64-70. https://doi.org/10.2214/AJR.12.9196

Johnson, T.R.C., M. Sedlmair., D. Morhard., C. Fink., S. Weckbach., M.F. Reiser., C.R. Becker. (2007): Material differentiation by dual energy CT: initial experience. *Eur Radiol, 17*, 1510-1517. https://doi.org/10.1007/s00330-006-0517-6

Judith E. Adams. (2008): *Dual energy X-Ray absorptiometry*. University of Manchester, Oxford Road, Manchester. https://doi.org/10.1371/journal.pone.0091904

Leni Aziyus Fitri. (2015). *Pengelompokan batu urinary berdasarkan nilai HU berbasis dual energy micro CT skyScan 1173* (Master Thesis). Institut Teknologi Bandung.

Li, X.H, R. Zhaou, B.Liu, Y.-Q. Yu. (2013): Determination of urinary stone composition using dual energy spectral CT: Initial in vitro analysis. *Journal of Clinical Radiology, 68*, 370-377. https://doi.org/10.1016/j.crad.2012.11.022

Paul.J, Ralf W. Bauer a, Werner Maentele b, Thomas J. Vogl. (2011). Image fusion in dual energy computed tomography for detection of various anatomic structures–Effect on contrast enhancement, contrast-to-noise ratio, signal-to-noise ratio and image quality. *European Journal of Radiology (80),* 612–619. https://doi.org/10.1016/j.ejrad.2011.02.023

Primak, N Andrew, Terri J. Vrtiska, Mingliang Qu, & Cynthia H. McCollough. (2011). *Kidney stone.* Springer-Verlag Berlin, Jerman. https://doi.org/10.1007/978-3-642-01740-7

Pydi Kavita, Daisy Rani Alli, Annepu Bhujanga Ra. (2022). Study of image fusion optimization techniques for medical applications. *International Journal of Cognitive Computing in Engineering 3,* 136–143. https://doi.org/10.1016/j.ijcce.2022.05.002

Ramos, R.M. Lorente, J.A. Arman, N. Galeano, A. Munoz H, J.M Garcia Gonzales, dan J.G Molinero. (2011). Dual energy X-ray absorptimetry: Fundamentals, methodology, and clinical applications. *Journal of Radiologia, 54*, 410-423. https://doi.org/10.1016/j.rx.2011.09.023

Sfoungaristos, Kavouras A, Katafigiotis I, Perimenis P. (2012). Role of white blood cell and neutrophil counts in predicting spontaneous stone passage in patients with renal colic. *BJU Int*;110:339-345. https://doi.org/10.1111/j.1464-410X.2012.11014.x

Tabari A, Lo Gullo R, Murugan V, et al. (2017). Recent advances in computed tomographic technology: cardiopulmonary imaging applications. *J Thorac Imaging ;32(2*).

Thomas, C., O. Patschan, D. Ketelsen, I. Tsiflikas, A. Reimann, H. Brodoefel, M. Buchgeister, U. Nagele, A. Stenzl, C. Claussen, A. Kopp, M. Heuschmid, H.P. Schlemmer. (2009). Dual energy CT for the characterization of 49 urinary calculy: In vitro and in vivo evaluation of a low-dose scanning protocol. *Eur Radiol, 19*, 1553-1559. https://doi.org/10.1007/s00330-009-1300-2

Zaidi, et al. (2006). *Attenuation correction strategies in emission tomography: Quantitative Analysis in Nuclear Medicine Imaging.* Springer US, Boston, MA.